

Mechanical Responses of Membranes probed with Force Spectroscopy

Rate dependence of the membrane deformation via tether pulling



A thesis submitted towards partial fulfilment of BS-MS Dual Degree Programme

By

Roshni Bano

under the guidance of

Dr. Thomas Pucadyil

Assistant Professor, Biology Division

Indian Institute of Science Education & Research (IISER) Pune

Certificate

This is to certify that this thesis entitled 'Mechanical Responses of Membranes probed with force spectroscopy' towards the partial fulfillment of the BS-MS dual degree programme at the Indian Institute of Science Education and Research (IISER), Pune represents original research carried out by Roshni Bano at IISER Pune under the supervision of Dr. Thomas Pucadyil, Assistant Professor, Biology Division, IISER Pune during the academic year 2012-2013.

Dr. Thomas Pucadyil

Assistant Professor, Biology Division

Biology Division, IISER Pune

Declaration

I hereby declare that the matter embodied in the thesis entitled 'Mechanical Responses of Membranes Probed with Force Spectroscopy' are the results of investigations carried out by me at the Biology Division, IISER Pune under the supervision of Dr. Thomas Pucadyil, Assistant Professor, Biology Division, IISER Pune. The same has not been submitted elsewhere for any other degree.

Roshni Bano

BS-MS Dual Degree Student

IISER Pune

I. Abstract

Mechanical properties of membranes such as surface tension and elastic constants play an important role in cellular processes such as vesicular transport and cell migration. Conventionally, these parameters have been calculated by deforming the membrane into cylindrical nanotubes ('membrane tethers') using shear flow and micropipette aspiration. In recent times, more sensitive approaches involving optical traps and force spectroscopy have been used to measure forces involved in and determine energetic parameters of the tether pulling process. Here, we report our observations from constant speed tether-pulling experiments using force spectroscopy on mammalian cells in culture. Tethers pulled at a constant speed appear to relax in a discrete, step-wise manner. Strikingly, such experiments carried out with model membrane systems also display similar force profiles, suggesting that such a mechanical response may be an inherent property of the lipid bilayer. Importantly, we observe a pulling rate dependence of the characteristic parameters of force profiles obtained on both cell and model membranes. We interpret these results to reflect a transition of the lipid bilayer from a viscous to a viscoelastic regime, caused by an increase in pulling rate. Further, we focus on the rate dependence of a particular parameter of the force curve called the 'tether force' that provides a measure of the resistance offered by the membrane to deformation. Subtle differences in this rate dependence seen in cell and model membranes are currently under investigation. Our results suggest that physical parameters defining membrane behaviour need to be interpreted in the context of the timescale of membrane deformation.

I. List of Figures

Page 15 : Figure 3.1 : Tether pulling experiment on HeLa cell membranes

Page 16 : Figure 3.2 : Characterisation of planar 'spill' supported bilayers

Page 17 : Figure 3.3 : Tether pulling force curves on planar 'spill' supported bilayers

Page 18 : Figure 3.4 : Giant Unilamellar Vesicles (GUV)s

Page 18 : Figure 3.5 : Tether pulling force curve on ruptured GUV membranes

Page 20,21 : Figure 3.6 : Pulling rate dependence trends obtained on cell membranes

Page 21,22 : Figure 3.7 : Pulling rate dependence trends obtained on supported bilayers

Page 23 : Figure 3.8 : Refined pulling rate dependence trends in tether force obtained on cell membranes

Page 23 : Figure 3.9 : Refined pulling rate dependence trends in tether force obtained on supported bilayers

Page 24 : Figure 3.10 : Pulling rate dependence trends in tether force obtained on ruptured GUV membranes

Page 24 : Figure 3.11 : Pulling rate dependence trends in tether force obtained on mica supported bilayers

Page 25 : Figure 3.12 : Refined pulling rate dependence trends in tether force obtained on supported bilayers with a stiffer cantilever

Page 27 : Figure 3.13 : Relaxation trace for a tether pulled from a cell membrane

Page 27 : Figure 3.14 : Relaxation trace for a tether pulled from a supported bilayer

II. List of Tables

Page 19 : Table 3.1 : Summary of tether pulling experiments

Acknowledgments

To start with, I would like to thank my supervisor, Dr. Thomas Pucadyil for being an incredible source of support and encouragement throughout the course of this project. I am deeply grateful to him for insisting that I decide the direction to take in the project, but at the same time giving me the space and time to get things working. His enthusiasm at finding something new and interesting, however trivial, served as consolation for many a day when nothing would work. Through our discussions on the 'right' experiment to do, I have learnt a great deal about how to approach a scientific problem effectively. I can particularly remember this one instance, where I was convinced that the experiment hadn't worked, but he saw it in a new light that inspired a whole month's work! Science apart, I couldn't have wished for a nicer, funner supervisor!

I would also like to thank Dr. Shivprasad Patil, my unofficial co-supervisor. In this project, where I would have to shuttle from one lab to another quite regularly, he tried to make sure that things went as smoothly as possible. I can remember many occasions, when I would argue incessantly over some point of experiment design, but he would listen patiently and explain until I was convinced. And of course, he was kind enough to help me out whenever I needed help trouble shooting a technical issue or interpreting the newest data set.

Thanks are due to Murthy, who taught me everything I know about operating the AFM and for rushing to the lab at odd hours when I would call and complain about apparent instrument misbehaviour. Also, I would like to thank Sachin, Srishti and Manish – there was never a dull moment in lab with any of you around. Thanks for listening to me crib endlessly and cheering me up on all those bad days!

This acknowledgement wouldn't be complete without mentioning all my friends at IISER for making these five years (especially the final one!) an unforgettable, amazing experience. Last, but not the least, my parents! For giving me the freedom to chase my dreams and never doubting my capabilities, even at times when I wouldn't be too sure of myself!

1. Introduction

Mechanical properties of membranes have been the focus of active interdisciplinary research in the last century. Membranes represent an interesting class of material in the physical sciences, given their self assembly properties and dynamic structure at a molecular level. In the biological sciences, membranes were initially looked at, primarily, as compartmentalising barriers that maintain cellular and organelle identity. However, membranes have now been conclusively shown to be significant and active contributors to cellular function, for instance, by providing a surface for reactions involved in cell signalling and vesicular transport. These functions are modulated depending on the chemical identity of the lipids constituting the membrane. However, membranes are also characterised by physical properties, specifically mechanical properties, which are also thought to impinge on membrane function.

One such mechanical property of the membrane which has been studied in great detail is membrane tension. Membrane tension can be related to the force required to deform the membrane. Using a number of experimental techniques to affect the value of membrane tension in cellular systems, it has been found that membrane tension can affect cellular function (Sheetz & Dai, 1996). For instance, vesicular trafficking is modulated depending on the tension in the cell membrane. Broadly speaking, increasing membrane tension seems to stimulate exocytosis, while decreasing membrane tension favours endocytosis (Dai et. al., 1997; Dai & Sheetz, 1995). There do exist however, exceptions to this paradigm (Apodaca, 2002). Also, the phenomena of cell spreading and cell motility have been found to be affected by membrane tension (Raucher & Sheetz, 2000; Keren, 2011). These findings seem to indicate that membrane tension may be regulated by the cell within a certain range and that tension itself may serve as a regulatory factor for various cellular functions. Exactly how this process is coordinated in the cell is not completely understood (Diz-Munoz et. al., 2013). One hypothesis is that cellular surface area might be regulated in order to regulate membrane tension (Morris & Homann, 2001). Efforts to test this hypothesis in a cell membrane mimetic system have yielded some useful insights. It has been observed that these membranes respond to expansion strain by adsorbing lipid vesicles and compression strain by tubule expulsion (Staykova et. al., 2011).

The same results are recapitulated using a theoretical model which allows the bilayer to reach its lowest energy state under various perturbations (Staykova et. al., 2013). These observations, remarkably, are in agreement with the effects seen on vesicular transport on perturbing tension in cell membranes. Hence, this approach of integrating observations from membrane deformation experiments in cellular and cell free membrane systems, coupled with theoretical modelling has been greatly illuminating with respect to the regulation and role of tension in cell membranes.

While membrane tension is one mechanical property of interest, there are several other physical properties that characterise membranes. These include the shear modulus of the membrane, which is quite low owing to the fluid nature of the lipid bilayer (Evans, 1973; Henon et. al., 1999) and the stretch modulus which is quite high due to the aversion of the bilayer to areal stretching (Hochmuth & Waugh, 1987). Also, of interest are the viscosity of the membrane (Hochmuth & Waugh, 1987) and its bending stiffness (Waugh et. al., 1992), which is the resistance offered by the membrane to a change in curvature. All these parameters have been obtained from experiments performed on erythrocyte membranes.

A powerful method to measure these material properties is via deformation of the membrane to produce nanoscale cylindrical tubes called membrane tethers. Membrane tethers can be formed from the cell surface by shearing using a fluid flow (Hochmuth, Mohandas & Blackshear 1973), aspirating with a micropipette (Hochmuth & Evans I, 1982) and extruding using optical tweezers (Dai & Sheetz, 1998). These techniques have been used to study the process of tether formation in cell membranes (Raucher & Sheetz, 1999) and reconstituted membranes such as giant unilamellar vesicles (Bo & Waugh, 1989). Analysis of these tether pulling experiments allows one to measure the force required to form a tether (Hochmuth & Evans I, 1982) and analyse its dependence on material properties of the tether and experimental variables such as tether pulling velocity and hydrostatic pressure (Hochmuth & Evans II, 1982). While experiments performed on cell membranes do not allow lipid bilayer properties to be studied independent of the effect of cellular components such as the cytoskeleton and membrane proteins, it is possible to do this in membrane mimetic systems such as giant unilamellar vesicles (Bo & Waugh, 1989) and supported bilayers. For a long time, however tethers were thought to be devoid of cytoskeletal components (Raucher et. al., 2000) and thus tethers pulled

from cell membranes and membrane mimetic systems *in vitro* were thought to be similar, in spite of obvious differences in the organisation and composition of these membranes. However, a recent study showed that tethers pulled from cell membranes do contain actin (Pontes et. al., 2011), suggesting an added complication in tether pulling experiments performed on cell membranes. Membrane tethers have also recently been simulated in order to understand the process of tether formation (Baoukina et. al., 2012). All in all, membrane tethers constitute a suitable system in which membrane deformation can be carried out and the mechanical properties of membranes playing a role in this process can be investigated.

Currently, using optical tweezers is by far the most widely used technique in order to pull out membrane tethers. The force transducing and force detecting probe in this system is a micron sized bead, which can be manipulated using a focussed laser light. The wide usage of the technique stems from its versatility in experimental design and sensitivity of force measurement - 0.1 pN (Neuman & Block, 2004; Kuo & Sheetz, 1992). However, in the last decade, the use of atomic force microscopy (AFM) as a tool to study cell surface/membrane properties at the single cell/molecule level has been gaining popularity (Muller et. al., 2009). The basic principle behind the working of this technique is force measurement via a force detecting 'tip' loaded on to a spring like 'cantilever'. The movement of this 'cantilever tip' can be controlled using a sophisticated system of piezoelectric motors. The deflection of (a laser spot focussed on) the cantilever tip in response to applied forces can be tracked with the help of a finely tuned photo-detecting apparatus. The deflection of the cantilever tip can then be related to the force experienced by the cantilever. While the force sensitivity of AFM (~1 pN) is slightly lower compared to optical tweezers, the advantages offered by this device are its amenability to (physical and chemical) modification of the force detecting probe as per need and the wide range of detectable forces (pN to hundreds of nN); optical tweezers work within a much narrower range.

In this work, we have attempted to study mechanical responses of membranes by pulling tethers using AFM based force spectroscopy. The basic force spectroscopy experiment consists of establishing contact with the membrane via the cantilever tip and pulling away the cantilever in order to form a tube of membrane. The apparatus

allows one to record the force experienced by the cantilever tip (which is a measure of the force exerted by the membrane tether) during the entire process of pulling a tether. The experimental data is obtained in form of a plot called the 'force curve' that shows the force detected by the cantilever tip versus the separation between the cantilever tip and the membrane surface. Force curves have been obtained in this manner on cell membranes (of HeLa cells) and membrane mimetic systems (supported bilayers, ruptured giant unilamellar vesicles). These force curves have been analysed for parameters that can be related to mechanical properties of membranes. Comparisons between these parameters have been made for cell membranes and supported bilayers for various experimental conditions. One set of experiments that we have focussed on is the analysis of the rate dependence of the tether pulling process (in terms of the parameters of the force curves). Strikingly, we see a similarity not only in the appearance of the force curves obtained on cell membranes and supported bilayers, but also in the trendlines of force curve parameters with pulling rates in both cell membranes and supported bilayers. While some of these results have so far not been reported in literature, the others have not been investigated in great depth. We believe that these force spectroscopy experiments have thrown light on some novel mechanical properties of membranes and offer us an opportunity to revisit the idea of how mechanics of membranes can affect membrane function.

2. Materials and Methods

(i) Membrane systems

(a) *Cell culture and sample preparation* : HeLa cells were grown in monolayers on glass coverslips (Ted Pella Inc.) in 35 mm petridishes at 37°C in 5% CO₂ in DMEM; Dulbecco's Modified Eagle's medium (Lonza) containing 10% FBS; Fetal Bovine Serum (Gibco) and 0.02 % Penicillin/Streptomycin for 48 hours prior to the start of the experiment. In order to obtain a single layer of cells in culture, a confluent culture was treated with 0.25% Trypsin-EDTA (Gibco), detrypsinised in DMEM containing 10% FBS and seeded at a density of 80000 cells/coverslip.

(b) *Small unilamellar vesicle (SUV) preparation* : Glass tubes were cleaned with 1% SDS (Sodium Dodecylsulphate), rinsed thoroughly with MilliQ water, followed by methanol and chloroform. Lipids were aliquoted from chloroform stocks (from Avanti Polar Lipids) into the clean glass tube and mixed gently. For all the experiments described in this thesis, liposomes composed of DOPC (1,2-dioleoyl-glycero-3-phosphocholine): DOPS (1,2-dioleoyl-glycero-3-phospho-L-serine) : RhPE (1,2-dioleoyl- sn-glycero-3-phosphoethanolamine-N-(lissamine rhodamine B sulfonyl) in 84:15:1 mol% or 84.5:15:0.5 mol% were used. The solvent (chloroform) was air - dried. The glass tube containing the lipids was then left in high vacuum for 30 minutes at 50°C for further drying. The lipids were hydrated in MilliQ water either for 30 minutes in a 50°C water bath with intermittent vortexing or overnight at room temperature. The hydrated lipids were sonicated with a probe sonicator at 30% amplitude for 5 minutes (2 second pulses interspersed with 3 second gaps) to generate small unilamellar vesicles. During sonication, the glass tube was placed in an ice water mixture. After sonication, the sample was centrifuged at 20,000 g for 20 minutes at room temperature and the supernatant was collected & stored at 4°C. These SUVs were used to prepare various model membrane systems described here.

(c) *Supported Bilayers with Excess Membrane Reservoir (SUPER) template preparation*: Silica beads (5 or 20 μm diameter from Corpuscular Inc.) were added to solution containing 200 μM liposomes and the desired NaCl concentration in a total volume of 100 μL in a 1.5 mL siliconised Microcentrifuge tube (Starlab). This reaction mixture was incubated in the dark at room temperature for 30 minutes. The templates formed were washed four times with 1 mL water, each time followed by a 300g spin in a swinging bucket rotor at room temperature, leaving 100 μL of water after each wash.

(d) *Giant unilamellar vesicle (GUV) preparation* : These vesicles were prepared by electroformation. 15 μL each of chloroform solution containing 1 mM total lipid composed of DOPC (1,2-dioleoyl-glycero-3-phosphocholine): DOPS (1,2-dioleoyl-glycero-3-phospho-L-serine : RhPE (1,2-dioleoyl- sn-glycero-3-phosphoethanolamine-N-(lissamine rhodamine B sulfonyl) in 84:15:1 mol% was applied on two clean Indium Tin Oxide; ITO coated glass slides (Delta Technologies) and air dried. The slides were dried further in a vacuum dessicator for 60 minutes. They were then clamped (with the sides containing the dry lipid film facing each other) with a spacer in between to form a chamber. This chamber was filled with 320 mM sucrose solution. Copper strips wrapped around the ends of the glass slides were used to apply an AC peak-to-peak voltage of 4 V, 10 Hz for 90 minutes. At the end of this process, the sucrose solution containing GUVs was stored at 4°C and used within a day.

(ii) Sample preparation for AFM

(a) *HeLa cells* : The cells were washed with either HEPES buffered HBSS (Hanks' balanced salt solution; 137 mM NaCl, 5.4 KCl, 5.6 mM glucose, 0.8 mM MgSO_4 , 1.3 mM CaCl_2 and 10 mM HEPES) or L15 cell culture medium (Gibco). The coverglass supporting the cells was placed in the AFM sample holder. The cells were washed once more with the chosen buffer and equilibrated in the sample chamber at room temperature for 45-60 minutes. While we initially used HEPES buffered HBSS, L15 was preferred for these experiments to enable the cell to

survive better in the course of the experiment in a non-CO₂ environment.

(b) *SUPER templates*: A glass coverslip was rinsed with methanol, air-dried and fixed into the AFM sample holder. In order to coat the glass surface, an appropriate volume of 2 mg/mL BSA (Bovine Serum Albumin) solution in HBS (HEPES buffered saline; 150 mM NaCl, 20 mM HEPES) was incubated on the glass surface for 10 – 15 minutes. The freshly formed coating was washed with HBS 2-3 times and finally submerged in HBS. SUPER templates prepared in 1M NaCl on 20 μm silica beads were deposited onto this BSA coated glass coverslip in the AFM sample holder containing HBS.

(c) *Planar 'spill' bilayers*: Glass coverslips were etched in 1M KOH by sonication with a probe sonicator at 60% amplitude for 10 minutes (1 second pulses interspersed with 2 second gaps). The coverslips were then washed with milliQ water to remove KOH and dried in a vacuum dessicator for 30 minutes. These dry coverslips were then subjected to plasma treatment (using an Emitech K1050X Plasma Asher) in order to make them hydrophilic.

In order to prepare 'planar spill bilayers', SUPER templates prepared in 1M NaCl on 5 μm silica beads were allowed to spill their excess reservoir on a glass coverslip submerged in HBS (which was fixed in the AFM holder and treated in the manner described above). Once the spill bilayers reach a stable size (after ~10 -15 minutes), the AFM sample holder is tapped gently to shake away the silica beads trapped under the spill, without damaging the spill itself. The solution was allowed to thermally equilibrate for ~ 10 minutes and then the experiment was begun. The hydrophilicity of the glass surface used for spillage is quite critical to obtain bilayers that behave similarly everytime this procedure is used.

Spill bilayers were also prepared on mica substrates. A freshly cleaved piece of mica (Electron Microscopy Sciences) was placed in the AFM sample holder and exactly the same procedure described above for preparing spill bilayers on glass was used.

(d) *Ruptured GUVs* : A glass coverslip was cleaned and coated with BSA, with the same procedure as that described for preparing SUPER templates for AFM. GUVs (containing 320 mM sucrose inside) were allowed to rupture on a BSA coated coverslip in milliQ water. After an incubation time of ~15 minutes to allow for the ruptured vesicles to settle on to the surface, a stock of buffer of the appropriate concentration was added to bring the solution osmolarity to that corresponding to 1x HBS.

Note : All model membrane systems used for experiments described here have the same composition, DOPC : DOPS : RhPE = 84 : 15 : 1 mol%.

(iii) **Force spectroscopy experiments**

The atomic force microscope Nanowizard II used in these experiments was acquired from JPK instruments. The AFM sample holder was placed on the stage of an inverted microscope. This allowed for easy visualisation of the sample and the positioning of the cantilever on the point/area of interest. Silicon nitride contact mode cantilevers (MikroMasch CSC38/AIBS) were rinsed in water, followed by methanol and finally cleaned with a UV- ozone cleaning system (Novascan) for 30 minutes. Each cantilever cleaned this way was used for ~ five experiments, after rinsing with water and methanol before each experiment. The cantilever was calibrated before each experiment using thermal noise amplitude analysis (Hutter & BechHoefler, 1993) to determine its sensitivity and spring constant. The measured spring constant of the cantilevers used for most experiments lay between 20 – 80 mN/m (the range specified by the manufacturer), with a typical value of 50 mN/m.

The protocol for carrying out the basic tether pulling experiment was the following: The cantilever tip was brought close to the membrane surface at

a constant speed until a repulsive force of 500 pN (called the 'relative set point') was reached. Contact (at a constant force) was maintained with the surface for 10s. The cantilever tip was retracted from the surface (at the same speed as the approach) leading to the formation of a membrane tether. The retraction was continued until the cantilever tip reached the zero force (deflection) baseline. Throughout this process, the force experienced by the cantilever was monitored along with its height above the sample surface.

All force curves reported in the 'Results' section for cell membranes, supported bilayers and ruptured GUVs were obtained by continuously probing the surface at one point. The force curves obtained on SUPER templates were obtained by sampling multiple points over an area of 500 nm x 500 nm.

In order to perform a pulling rate dependence trend, tethers were pulled from the membrane system of interest in the manner described above at the pulling rates of interest. The length to which the tether was pulled was changed based on the pulling rate, as was the sampling frequency of the instrument.

Tether relaxation time estimation

A few trial force curves were obtained at a particular pulling rate. The value of the average tether force at this pulling rate was calculated.

The membrane surface was approached at the desired pulling rate until a relative setpoint of 500 pN was reached. The cantilever tip was allowed to rest on the membrane surface for 10s at the constant relative set point force. A membrane tether was then pulled out until an attractive (corresponding to a downward force on the cantilever) set point of force was reached. This attractive setpoint was chosen to be less than the average tether force, in order to circumvent the possibility of step wise relaxation. Once the attractive set point was reached, the cantilever movement was stopped and its decay back to the zero force baseline was

monitored in the force- time trace. This, we believe is a readout of the relaxation of the tether from a stressed to an unstressed state. Thereafter, the cantilever was pulled to a large distance away from the membrane in order to start another tether relaxation trial.

Tether relaxation time experiments in both cell membranes and supported bilayers were performed by probing at a single point on the membrane surface.

All force curves obtained in force spectroscopy were analysed using the JPK data processing software. The basic operations used to process all raw data included baseline correction (by using the furthest-from-sample-surface force value as the zero force value and subtracting it from the entire force curve), setting the point of contact of the cantilever tip with the surface as the 'zero height' and correcting for cantilever bending to calculate the true 'tip-sample separation'. In built functions were used to measure the force minimum corresponding to 'tether force' and detect 'steps' in force curves.

(iv) AFM imaging of planar 'spill' bilayers

This protocol for contact mode imaging of spill supported bilayers has been modified from Lin et. al., 2007.

Silicon nitride cantilevers used for force spectroscopy experiments were used for imaging as well. Cantilever cleaning and calibration was carried out as described previously. The cantilever tip was brought in contact with the sample with the system determined approach setpoint. The area to be imaged was chosen and a scanning force in the range 0.2 – 1 nN was used for imaging the bilayer. The imaging force was kept as low as possible to prevent damage to the sample.

(v) Fluorescence Microscopy

Epi-fluorescence imaging was performed using an Olympus IX71 inverted microscope. Images were acquired using Photometric Evolve EMCCD cameras. A xenon arc lamp (Lambda LS) was used as light source. All

images were acquired through either through a 60x or 100x oil immersion objective.

3. Results

(i) Tether pulling force curves obtained on various membrane systems

Tether pulling experiments on HeLa cell membranes

Force spectroscopy experiments were performed on cell membranes and supported bilayers as described in the 'Materials and Methods' section. Shown below (in Figure 3.1a) is a typical force curve obtained by pulling tethers from the membrane surface of a HeLa cell (adhered to a glass surface in L15 cell culture medium) at a pulling rate of 3 $\mu\text{m/s}$. The force curve corresponding to the 'approach' of the cantilever tip on the membrane surface is flat until it makes contact with the membrane surface (or more precisely, reaches the relative set point). The 'contact' corresponds to a steep increase in force. On approach, the cantilever tip is allowed to rest on the membrane surface for 10s in order to promote adhesion to the membrane. The force curve corresponding to the 'retraction' of the cantilever from the membrane surface shows a dip (called the 'tether force'), corresponding to the downward force exerted by a tether and possibly adhesion to the membrane surface. As the cantilever tip moves further away from the surface, the membrane tether relaxes in a step wise manner until the zero force baseline is reached. This could correspond to either a tether that is fully relaxed at this 'zero force' value or broken in the pulling process.

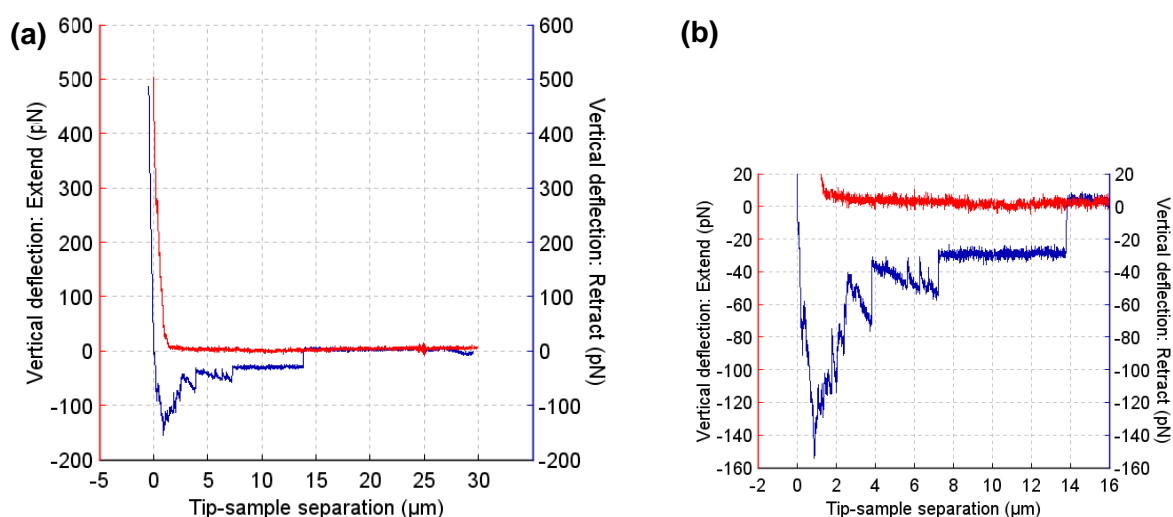


Figure 3.1 : Tether pulling experiment on HeLa cell membranes : (a) Force curves showing the approach of the cantilever tip to the cell surface (Red) and retraction of the cantilever tip from the surface (Blue). (b) A magnified plot of the force curve in Figure 3.1a showing the dip corresponding to tether force and the step wise relaxations. Again, the approach curve is Red and the retraction curve is Blue.

Tether pulling experiments on supported bilayer systems

The same tether pulling experiment at a pulling rate of 3 $\mu\text{m/s}$ was performed on supported bilayers (DOPC:DOPS:RhPE = 84:15:1 mol%). Supported bilayers were prepared from the spillage of excess reservoir of a SUPER template (prepared in 1M NaCl) on a glass surface in HBS buffer. SUPER templates used for preparing ‘spill’ bilayers were made in 1M NaCl because the membrane reservoir accumulated on the template increases with increasing salt concentration used in the reaction mix (Pucadyil & Schmid, 2010). Templates prepared in 1M NaCl have enough reservoir to produce reasonably sized spills that can be probed using the cantilever tip.

These spill bilayers have been characterised using fluorescence microscopy and AFM imaging. They appear to be uniform both in terms of fluorescent intensity and height profiles (as is visually discernible in the figure below, Figure 3.2). The height profile (Figure 3.2c) however, confirms that these ‘spills’ are indeed bilayers. Their height above the surface is 3-4 nm. The major constituent of these bilayers is the DOPC lipid and DOPC bilayers are known to have a thickness of ~ 3 nm.

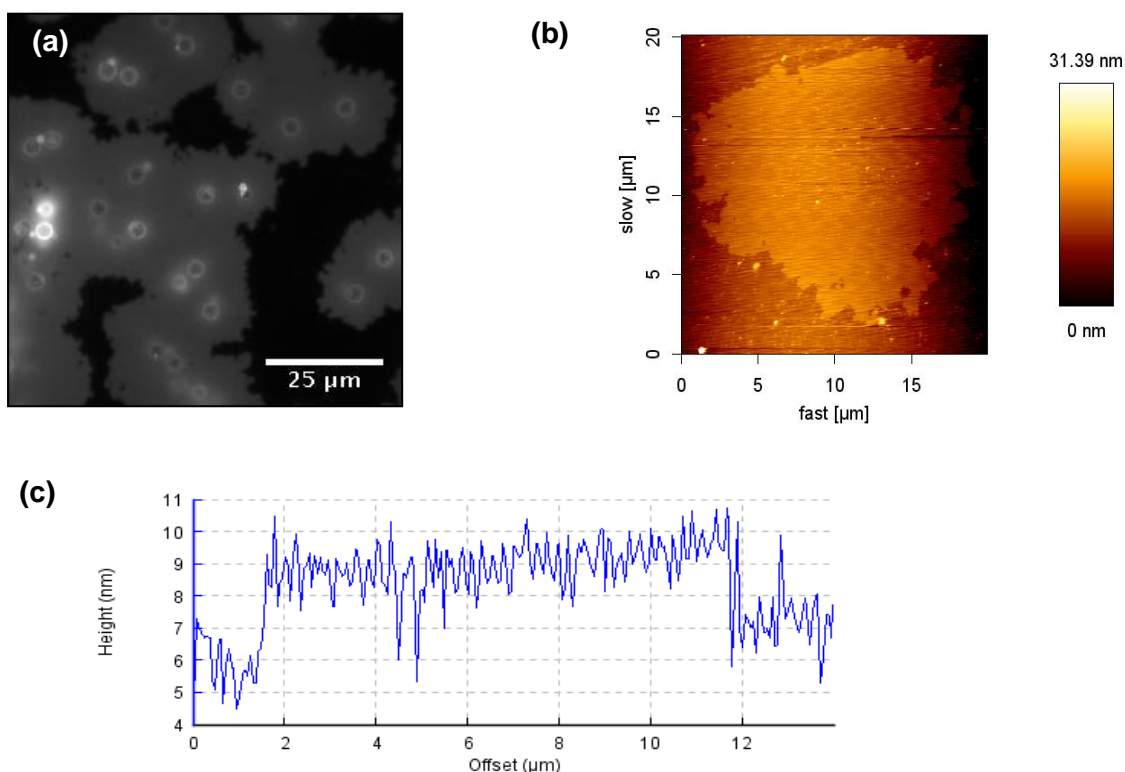


Figure 3.2 : Characterisation of planar ‘spill’ bilayers (a) Fluorescence image of a ‘spill’ containing labelled lipid (bright circles are 5 μm silica beads) (b) AFM image of a spill (c) Height profile along an edge from an AFM image of a spill.

The representative force profile from the tether pulling experiments on supported bilayers is shown below (Figure 3.3a). At first glance, this appears similar to the force profile obtained by pulling a tether from a HeLa cell membrane (Figure 3.1a), in terms of the presence of a 'dip' and step wise relaxations back to the zero force baseline in the retraction force curve. The typical force profile obtained by pulling tethers from SUPER templates of the same composition prepared in 1M NaCl is also similar to the HeLa cell force profile (data not shown).

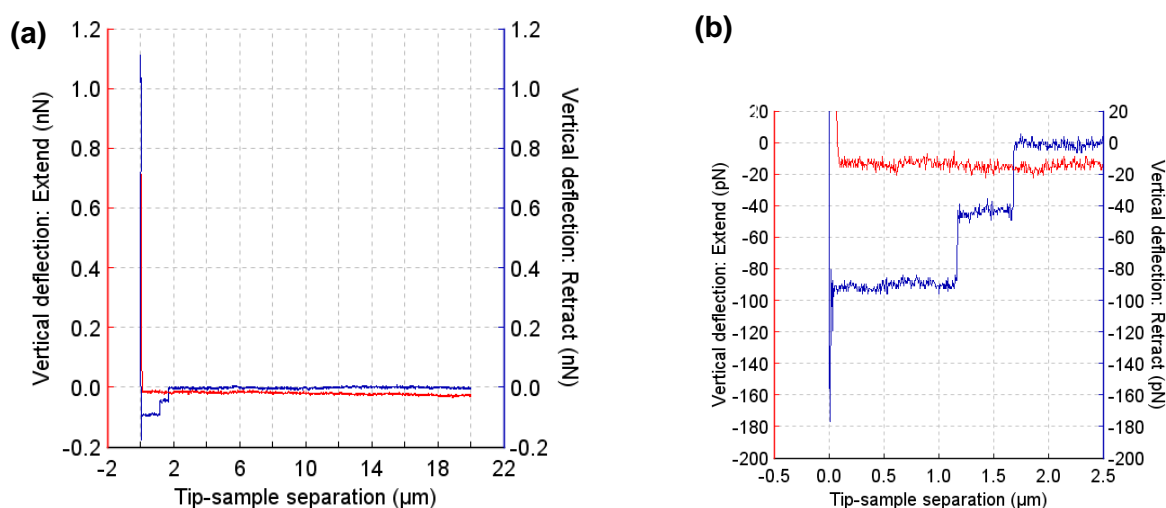


Figure 3.3 : Tether pulling force curves on planar 'spill' bilayers : (a) Supported bilayers composed of DOPC:DOPS:RhPE = 84:15:1 mol% were used. Force curves showing the approach of the cantilever tip to the membrane surface (Red) and retraction of the cantilever tip from the surface (Blue). (b) A magnified plot of the force curve in Figure 3.2a showing the dip corresponding to tether force and the step wise relaxations. Again, the approach curve is Red and the retraction curve is Blue.

However, subtle differences in the tether force minimum and the nature of the step wise relaxation do exist between cell membranes and supported bilayers. While the tether force minimum is sharp and thin for supported bilayers, it is broad and noisy for cell membranes. Also, the plateau preceding the step wise relaxation is generally flat in case of supported bilayers. However, in case of cell membranes, this plateau is often not flat. In effect, two kinds of step wise relaxations are seen in cell membranes, ones preceded by a flat plateau and ones preceded by a plateau with a finite slope.

Tether pulling experiments on ruptured GUV membranes

A Giant Unilamellar Vesicle (GUV; composed of DOPC:DOPS:RhPE = 84:15:1mol%) prepared by electroformation as described in the 'Materials and

Methods' section is shown in Figure 3.4 (a). Ruptured GUV membranes were prepared by adding the GUVs to hypo-osmotic medium (pure water) and allowing them to settle on a BSA coated glass surface. A representative picture of the ruptured GUV membrane is shown in Figure 3.4 (b). A tether pulling experiment on this ruptured GUV membrane at a pulling rate of 5 $\mu\text{m/s}$ showed the following force profile (shown in Figure 3.5). The retraction force curve in this force profile is noticeably different from those obtained on cell membrane and supported bilayers of the same composition. This is in terms of the magnitude of the 'dip' (which is much higher as compared to supported bilayers, at a pulling rate that is not very different) and the absence of step wise relaxations. However, this difference could have arisen due to a difference in the nature of the surface supporting the bilayer: while supported bilayers were prepared on glass, ruptured GUVs were deposited on BSA coated glass.

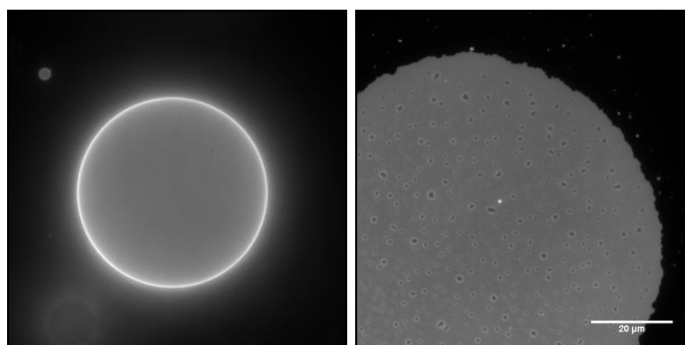


Figure 3.4 : Giant Unilamellar Vesicles (GUVs): (Left) GUV (DOPC:DOPS:RhPE = 84:15:1 mol%) containing labelled lipid visualised by fluorescence microscopy (Right) A ruptured GUV membrane immobilised on BSA coated glass in HBS.

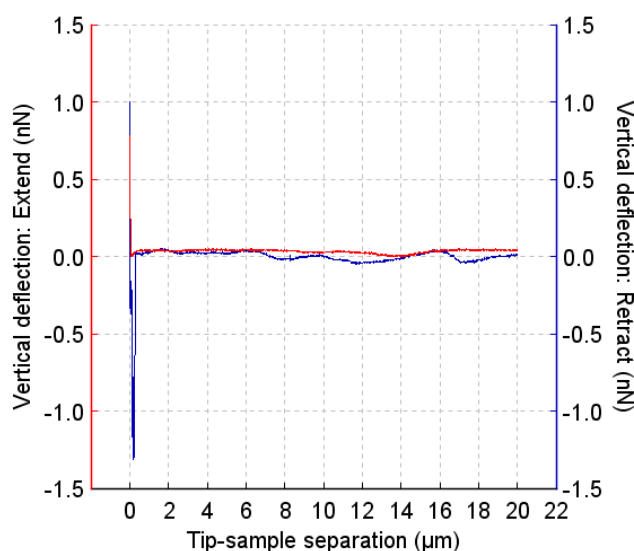


Figure 3.5 : Tether pulling force curve on ruptured GUV membranes: GUVs used were of the same composition as the 'spill' bilayers. Force curves showing the approach of the cantilever tip to the membrane surface (Red) and retraction of the cantilever tip from the surface (Blue).

A summary of the analysis of the force curves described above is given below.

Membrane system	Average tether force \pm Standard Deviation (nN)	Average step height \pm Standard Deviation (pN)
HeLa cell membranes	0.16 \pm 0.05 (N = 49)	34 \pm 11.9 (N = 49)
Planar spill bilayers	0.11 \pm 0.04 (N = 25)	50 \pm 8.1 (N = 25)
Ruptured GUV membranes	1.52 \pm 0.89 (N = 30)	No steps seen

Table 3.1 : Summary of tether pulling experiments : Tether forces and step heights observed on obtaining force curves on various membrane systems.

While we have good reason to believe that there exists a membrane tether when this experiment is performed, we have not actually visualised the tether pulling experiment in the current set up. When retraction force curves taken with identical parameters on a glass surface and a cell membrane surface are compared, only the force curves obtained on a membrane surface show stepwise relaxations. Also, if the cantilever tip is not allowed to rest on the membrane surface after approach, the force curves obtained do not show step wise relaxations. This suggests that the nature of the interaction of the cantilever tip with a glass surface is different from that with the membrane surface, possibly due to the presence of a membrane tether. Also, in literature, force spectroscopy experiments performed by Sun et. al. (Sun et. al., 2005) involving pulling tethers from cell membranes, the lipid bilayer labelled with quantum dots can be visualised in the process of tether formation. In these experiments, the existence of a tether pulled out using the AFM cantilever tip has been verified. We use similar AFM cantilevers in our experiments, and hence there is no reason to doubt that membrane tethers are indeed formed in these experiments.

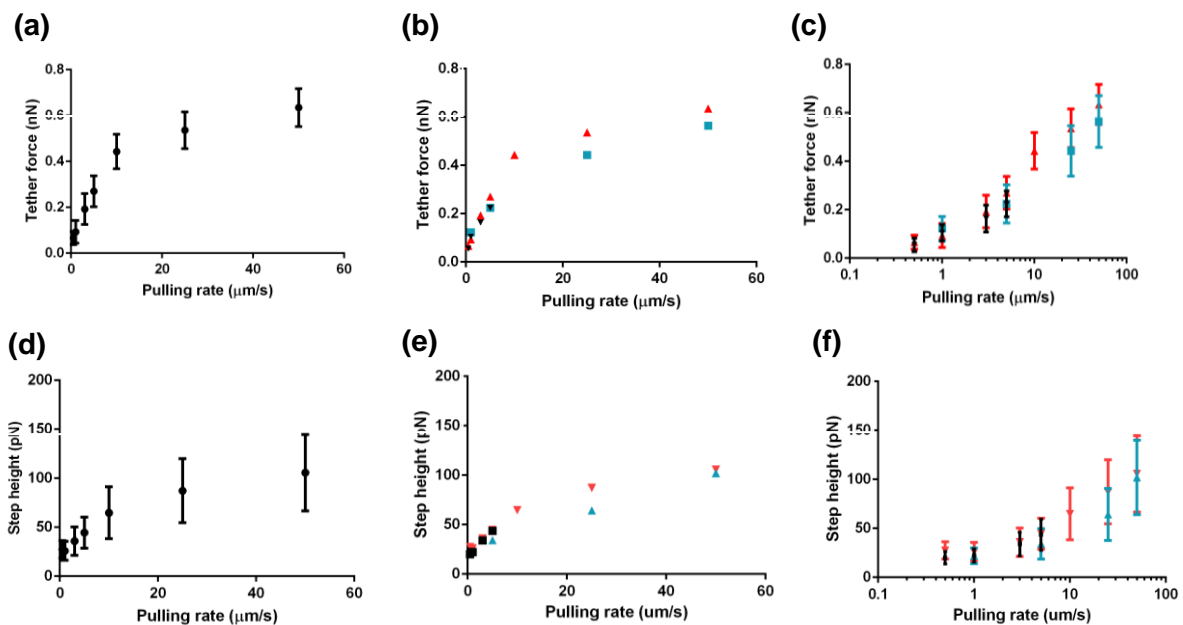
(ii) Pulling rate dependence experiments in various membrane systems

The presence of step wise relaxations and the dip in the retraction force curves are two very prominent features common to force profiles obtained from tether pulling experiments in both cell membranes and supported bilayers. In order to understand the origin of these features, experiments involving variation in the rates of pulling tethers were performed. The variation (with pulling rate) of three parameters of these force profiles was analysed:

- (a) **Tether force**, which is the magnitude of the ‘dip’ in the retraction force curve – this corresponds to the resistance offered by the membrane to pulling a tether, i.e. changing the shape of a flat membrane to turn it into a cylindrical tube
- (b) **Step height**, which is the magnitude of each step wise relaxation
- (c) **Step probability**, which is the fraction of experiments where at least one stepwise relaxation is observed

Tether force trends in pulling rate dependence experiments on cell membranes

The following plots in Figure 3.6 show the variation of these three parameters in pulling rate dependence experiments performed on HeLa cell membranes. In general, the values for tether force and step height have been shown as mean values for a given experiment, with error bars showing the standard deviation about the mean. All three parameters – tether force (Figure 3.6a-c), step height (Figure 3.6d-f) and step probability (Figure 3.6g) show an increasing trend with increasing pulling rates. In the figure shown below, the leftmost panel has a representative trendline, while the two panels on the right have the pooled data for multiple trials shown on two different scales – a linear scale in the middle panel (error bars removed for clarity) and a logarithmic scale in the rightmost panel.



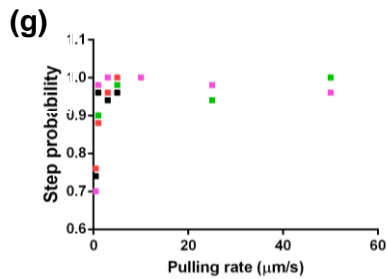
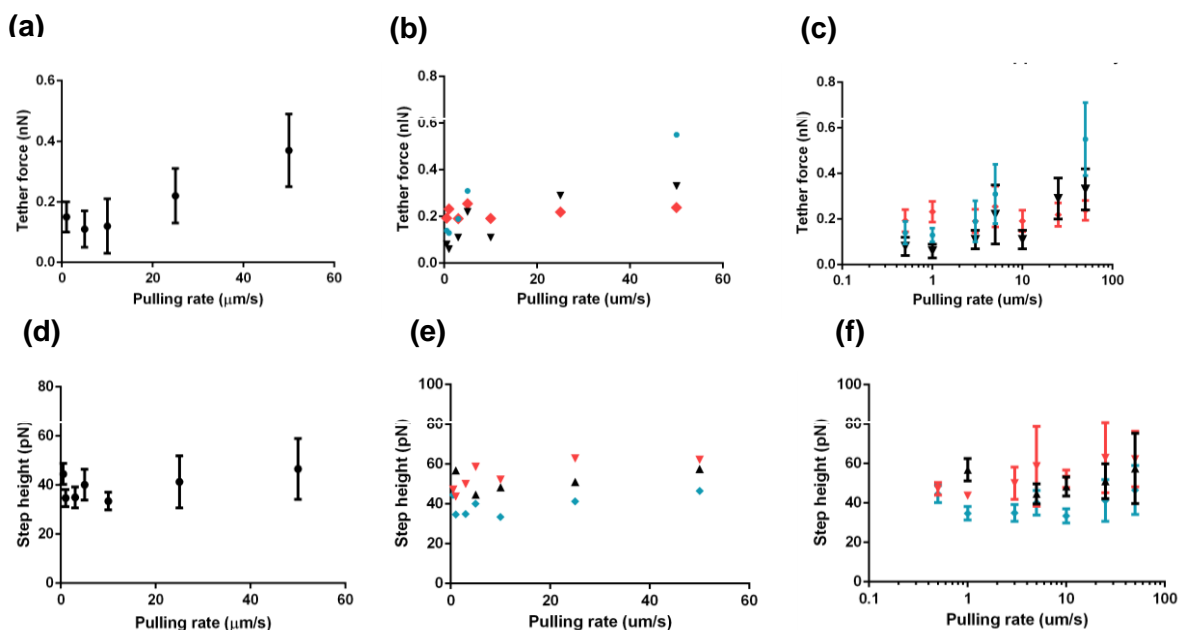


Figure 3.6 : Pulling rate dependence trends obtained on cell membranes (a) A representative tether force trend. Pooled tether force variation trends from multiple experiments (data points in different colours) on a (b) linear scale (c) logarithmic scale (d) A representative step height trend. Pooled step height variation trends from multiple experiments (data points in different colours) on a (e) linear scale (f) logarithmic scale (g) Pooled step probability trends from multiple experiments (data points in different colours).

The following plots in Figure 3.7 show the variation of the same three parameters (described previously) in pulling rate dependence experiments performed on supported bilayers (composed of DOPC:DOPS:RhPE = 84:15:1 mol%) prepared by spillage of excess membrane reservoir on glass. While tether force and step probability show an increasing trend with increasing pulling rates, step height remains fairly constant over this range of pulling rates. Again, the left most panel has a representative trend, while the two panels on the right have pooled data shown on two different scales.



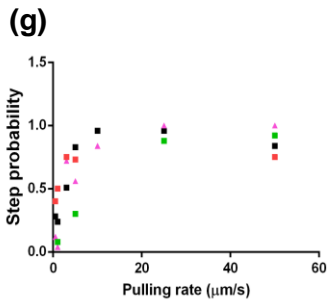


Figure 3.7 : Pulling rate dependence trends obtained on supported bilayers (a) A representative tether force trend. Pooled tether force variation trends from multiple experiments (data points in different colours) on a (b) linear scale (c) logarithmic scale (d) A representative step height trend. Pooled step height variation trends from multiple experiments (data points in different colours) on a (e) linear scale (f) logarithmic scale (g) Pooled step probability trends from multiple experiments (data points in different colours).

Interestingly, while force curves obtained on ruptured GUVs deposited on BSA coated glass surfaces showed no step wise relaxations in retraction force curve, even the tether force pulling rate dependence turned out to be quite different from that obtained from experiments on cell membranes and supported bilayers. In fact, there seems to be no dependence of the tether force on pulling rate. As mentioned in the previous section, this could arise from surface effects. In any case, this is an intriguing observation that we have tried to follow up on as described in the next subsection.

(iii) Exploring the origin of the tether force pulling rate dependence

Tether force is a parameter than can be used to arrive at significant material properties of membranes such as bending stiffness and membrane viscosity (Hochmuth & Evans, 1982 II). Hence, we tried to investigate in greater depth the nature of the tether force – pulling rate dependence trend by sampling over a logarithmic range of pulling rates separated by over two orders of magnitude.

Shown below in Figure 3.8 are the representative trendlines for the tether force pulling rate dependence obtained on HeLa cell membranes. In all of these trendlines, there seems to be a shallow inflection close to a pulling rate of $1\mu\text{m/s}$. In other words, the tether force rate dependence trend shows an “onset” around this pulling rate.

In order to reliably determine this onset rate (in all such trendlines that follow), the following method has been used : The trendline has been divided into two parts based on where there is a steep change in slope. The data points corresponding to each of the two parts have been fitted to a straight line (using linear regression). The intersection of these two lines is reported as the “onset rate” in each plot.

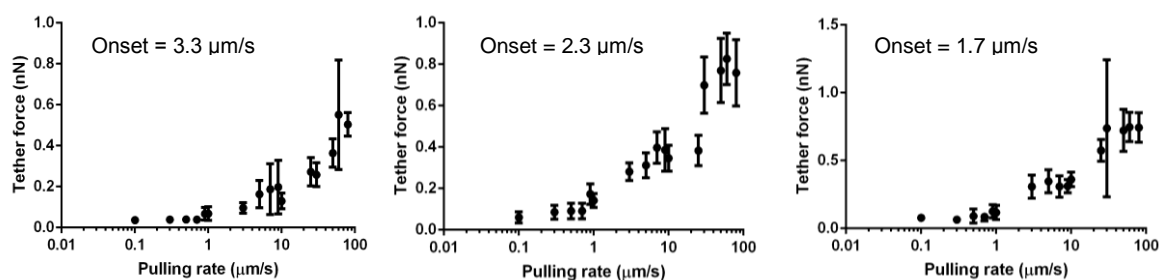


Figure 3.8 : Refined pulling rate dependence trends in tether force obtained on cell membranes : Three pulling rate dependence experiments carried out with the identical experimental procedure in order to look carefully at the variation of tether force with pulling rate for cell membranes.

Representative trendlines for the tether force pulling rate dependence obtained on glass supported bilayers (composed of DOPC:DOPS:RhPE = 84:15:1 mol%) are shown below in Figure 3.9. In all of these trendlines, there seems to be an onset around a pulling rate of 5- 10 $\mu\text{m/s}$.

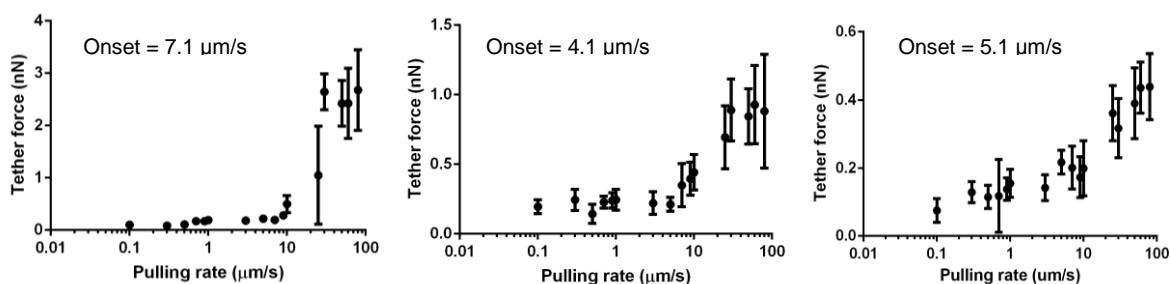


Figure 3.9 : Refined pulling rate dependence trends in tether force obtained on supported bilayers : Three pulling rate dependence experiments carried out with the identical experimental procedure in order to look carefully at the variation of tether force with pulling rate for supported bilayers.

Representative trendlines for the tether force pulling rate dependence obtained on ruptured GUV membranes (of the same composition as the supported bilayers used in the experiment described above, DOPC:DOPS:RhPE = 84:15:1 mol%) deposited

on a BSA coated glass surface are shown below in Figure 3.10. There seems to be no dependence of tether force on rates of pulling tethers.

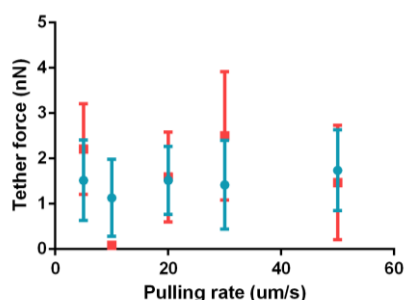


Figure 3.10 : Pulling rate dependence trends in tether force obtained on ruptured GUV membranes: Ruptured GUV membranes of the same composition as the supported bilayers, i.e. DOPC:DOPS:RhPE = 84:15:1 mol%. A smaller range of pulling rates was sampled, as there did not seem to be systematic variation in tether force with pulling rate.

Given that there was no tether force trend with pulling rate in force curves obtained on ruptured GUV membranes on BSA coated glass surfaces, we thought that the nature of the surface and the manner in which it interacts with the bilayer might affect the nature of the tether force trend observed with change in pulling rate. Hence, supported bilayers (of the same composition used before, DOPC:DOPS:RhPE = 84:15:1 mol%) prepared on atomically smooth mica supports (as against much rougher glass supports) were tested for their tether force pulling rate dependence. Only a few points in the entire range of pulling rates could be sampled for the mica supported bilayers due to technical constraints. As the comparative trendlines in Figure 3.11 show, the magnitudes of tether forces do not differ much between mica and glass supported bilayers, except at the highest pulling rate of 100 $\mu\text{m/s}$ (the coloured points show tether forces on a mica supported bilayer, the black points show a tether force trend on a glass supported bilayer). However, given the lack of datapoints, one cannot make any conclusive comments about the nature of the tether force rate dependence trend here, especially with respect to the presence of an inflection.

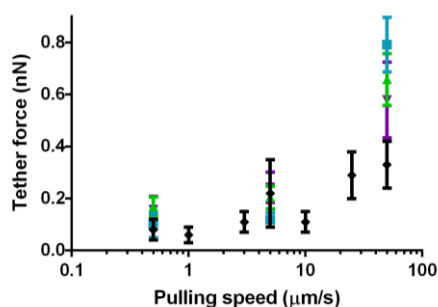


Figure 3.11 : Pulling rate dependence trends in tether force obtained on supported bilayers on mica substrates : Planar spill bilayers, of the composition DOPC:DOPS:RhPE = 84:15:1 mol% were used. The black points show a representative tether force trend for supported bilayers on glass. The coloured points show the values of tether force obtained for mica supported bilayers.

In order to verify that the tether force rate dependence that we observed in supported bilayers was not a cantilever dependent phenomenon, trendlines were obtained with a stiffer cantilever (typical spring constant ~ 0.15 N/m). These are shown below in Figure 3.12. Qualitatively, these seem to be no different than those obtained with the previous weaker cantilever (typical spring constant ~ 0.05 N/m). In two out of three of these tether force trendlines, the onset is around a pulling rate of $25 \mu\text{m/s}$. There does exist one trendline (on the left most panel of Figure 3.12) where the onset is close to $1 \mu\text{m/s}$. By and large, the onset is around the same order of magnitude pulling rate as seen for identical supported bilayers probed with a weaker cantilever (this value is $\sim 5 - 10 \mu\text{m/s}$).

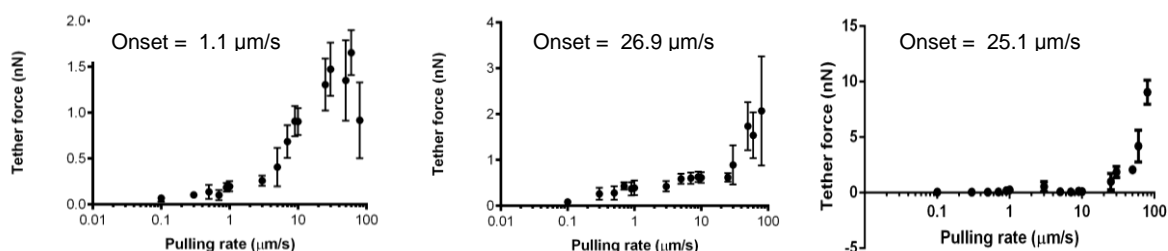


Figure 3.12 : Refined pulling rate dependence trends in tether force obtained on supported bilayers with a stiffer cantilever : Three pulling rate dependence experiments carried out with a stiffer cantilever in order to verify that the pulling rate dependence in supported bilayers (DOPC:DOPS:RhPE = 84:15:1 mol%) is not a cantilever dependent phenomenon.

In order to further investigate this tether force rate dependence, efforts are on to reproduce these results in a more standard supported bilayer system, prepared by adsorption and fusion of liposomes on to hydrophilic glass surfaces, rather than one prepared by spillage of excess membrane reservoir. Once this system is set up, it will be much more amenable than the previous one in terms of testing out the effect of changing parameters such as the nature of the surface, solution conditions and membrane composition on the tether force trend.

(iv) Estimating relaxation times of unperturbed membrane tethers

In the standard force spectroscopy experiment, a tether is continuously pulled from the membrane at a constant speed until it breaks/relaxes. In this process, in at least two membrane systems, an interesting tether relaxation profile is observed. However, this relaxation occurs under the application of force due to the movement of the cantilever tip at constant speed. We were interested in observing the relaxation of a tether when it is left free, unperturbed by cantilever forced movement.

This experiment is performed in the following way: the cantilever tip approaches the membrane surface till a repulsive set point (a force of 500 pN as in the standard tether pulling experiment) and is used to pull out a membrane tether until the downward (attractive) force experienced by the cantilever reaches a certain set point. The value of the latter set point was chosen based on the consideration that it should be less than the tether force at the pulling rate being used, otherwise, instead of the unperturbed relaxation which we are interested in looking at, the tether would probably relax in steps. Once this attractive setpoint was reached, cantilever movement was paused and the tether was allowed to relax. The relaxation curve was recorded as a force-time trace.

We expected to see an exponential relaxation of the cantilever (membrane tether) to the zero force baseline. This can be understood using the following idea : the rate of relaxation of the force (stress) experienced by the tether is proportionate to the force (stress) that the tether experiences at that instant. Hence, the relaxation of the force experienced by the membrane tether, F to a baseline force F_0 , with time t is given by:

$$F = F_0 (1 - e^{-t/T})$$

Hence, if the relaxation profile is fit to an exponential, one can obtain a characteristic relaxation time T .

However, relaxation profiles obtained from cell membranes did not fit well to a single or double exponential equation or even a $t/(1+t)$ and hence, characteristic relaxation times could not be determined. However, the time taken for the tethers to relax from the attractive set point to the zero force baseline was in the range of 100s of ms. Shown below in Figure 3.13 is a typical relaxation profile for a tether pulled from a cell membrane. The 'total' relaxation time does not seem to vary with the rate of pulling the tether to the attractive set point.

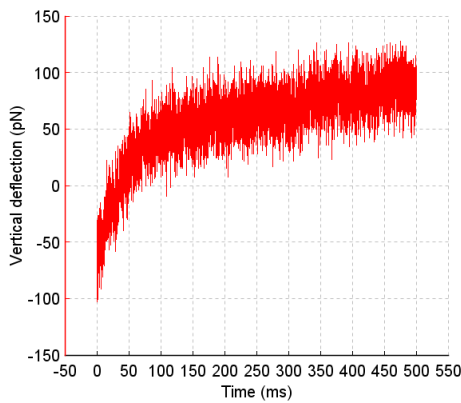


Figure 3.13 : Relaxation profile for a tether pulled from a cell membrane : Force-time relaxation trace for a tether pulled from a HeLa cell membrane to an attractive set point of 200 pN at a pulling rate of 5 $\mu\text{m/s}$ after pausing movement of the cantilever for 500 ms.

Relaxation profiles on supported bilayers were much more difficult to obtain. For reasons that we don't understand, tethers pulled from supported bilayers relax much before the attractive set point is reached, sometimes in steps. In rare cases however, when the tether doesn't relax before the attractive set point, relaxation profiles are obtained (representative profile shown in Figure 3.14). These look very different from those obtained from cell membranes. The major difference is in the magnitude of the 'total' relaxation time which lies within the range of 0.1- 10 ms.

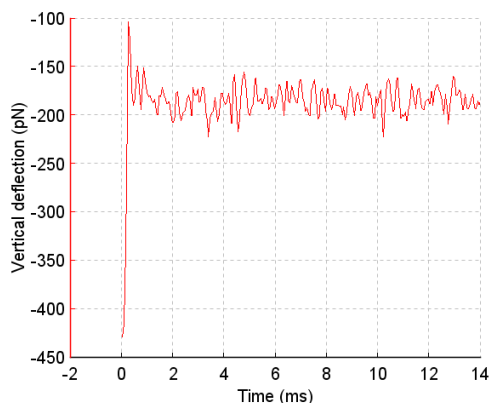


Figure 3.14 : A rare relaxation profile for a tether pulled from a supported bilayer : Force-time relaxation trace for a tether pulled from a supported bilayer to an attractive set point of 200 pN at a pulling rate of 5 $\mu\text{m/s}$ after pausing movement of the cantilever for 50 ms.

The motivation behind relaxation time estimation was to use this quantity to understand the intrinsic timescale of relaxation of the membrane systems of interest. With respect to this timescale then, one could consider the effect of the variation of the perturbation time scale of the system in order to understand the effect of pulling rate variation.

4. Discussion

(i) Similarities between tether pulling force curves obtained on various membrane systems

Force curves obtained at a particular pulling rate on cell membranes as well as a model membrane system show a striking similarity in appearance. In both kinds of force curves, a minimum corresponding to tether force is seen. Also, step wise relaxations while tether elongation are observed in both kinds of force curves. These broad similarities observed between complex cell membranes and simple model membranes (in spite of subtle differences when one looks closely at these features) suggest that this particular mechanical response of the membrane may be intrinsic to the lipid bilayer. On the other hand, the similar mechanical response could also result from a similarity in the effect of the 'support' on the lipid bilayer; in cell membranes, 'support' to the bilayer is provided by the cortical actin cytoskeleton.

A literature search shows that force curves obtained on pulling tethers from cell membranes of other cell types show similar features to the ones observed in our experiments. Interestingly, the magnitude of the average step height seems to be fairly constant (~ 30 pN) among different cell lines (including the one we have used in our experiments), bolstering the supposition that step wise relaxation may be a property inherent to the lipid bilayer. This value (or the appearance of the force curve obtained) is not affected when the cantilever tip used for tether pulling is modified chemically. However, the magnitude of the average step height as well as the spread in the distribution of the step height decreases when either the cellular actin cytoskeleton or glycocalyx is perturbed (Sun et. al., 2005). Changing membrane cholesterol concentration also affects the magnitude of the step height (Sun et. al., 2007).

In another study (Kocun & Janshoff, 2012), force spectroscopy experiments performed on 'pore spanning bilayers' (another model membrane system that attempts to mimic the cell membrane in terms of the presence of free standing patches of bilayer held down at a few points; Kocun et. al., 2011) show similar tether pulling force profiles to those obtained in our experiments. However, qualitative differences do exist in that there is no clear 'dip' seen in these force curves and that relaxation to the zero force baseline always occurs in a single step. Also, the part of

the force curve between the minimum and the 'step' is a flat line, which apparently corresponds to the presence of a membrane tube. This study also reports a change in the 'step height' with cholesterol addition to the model membrane.

Another interesting point to be made here is that while recent force spectroscopy experiments have yielded the kind of tether pulling force profiles described above, tether pulling force profiles obtained in experiments with optical tweezers are markedly different. These experiments have been performed in both cell membranes (Raucher & Sheetz, 1999) and model membranes - GUVs (Inaba et. al, 2005). While there does exist a steep increase in force corresponding to tether formation (this event has been visualised while the tether pulling experiment is carried out), tether elongation seems to correspond to a constant force plateau, unlike the step wise relaxation to zero force that is seen in AFM based force spectroscopy experiments.

(ii) Hypothesis to understand the origin of step wise tether relaxation

In the only other report of a step wise relaxation in a tether pulling experiment carried out on a model membrane system by Kocun et. al. (2012), the single 'step' observed in the force curve is interpreted as the force required to form the tether. This is not surprising, given the nature of this data.

In the experiments performed by Sun et. al. (2005), force profiles obtained on cell membranes show tether relaxation in multiple steps. These authors propose, hence, that the force minimum in tether pulling profiles corresponds to the formation of multiple tethers and that each step corresponds of breakage of a single tether.

We have our reservations about this interpretation of the tether pulling force profiles. This is mainly due to two reasons : a) It is not clear why the force value corresponding to the breakage of every single tether (pulled from cell membranes) should be a fairly constant value of ~ 30 pN; b) Estimates of tether diameter from micropipette based tether pulling experiments fall within the range of 10 – 500 nm. The contact diameter of the AFM cantilever tip, is only about tens of nms. Hence, we feel that it is unlikely that multiple membrane tethers can be pulled out with such a probe.

Since the diameter of membrane tethers is close to the diffraction limit of light, it is not possible to check for the presence of multiple tethers using light microscopy.

With this knowledge, we hypothesise that the 'step wise' relaxation in the force curve obtained while pulling a tether could result from the stick-slip motion of the lipid bilayer over the layer of water either trapped in the tether or between the bilayer and the support. In this purview, each 'step' corresponds to the 'slip' of the bilayer and the plateau before each step corresponds to the 'stick'. This could happen because as a tether is pulled, tension builds up in the membrane until it is relieved by slippage of the bilayer. This slippage can relieve the tension in the membrane by allowing release of membrane and increasing membrane area. In this framework, such slips could occur multiple times and reflect as multiple steps in the force curve.

The occurrence of stick-slip motion for a material like a lipid bilayer, which is considered to be a fluid, is quite unusual. Hence, it follows that the lipid bilayer could have some non-fluidic, solid like character. Materials with characteristics of both solids and liquids are known as viscoelastic materials (Banks et. al., 2011). Viscoelasticity is a property by virtue of which a material shows elastic behaviour like a solid (on application of stress, it has a memory of its original configuration and deforms proportionately to the applied stress) and viscous behaviour like a liquid (on application of stress, it deforms to relieve this stress, in a manner dependent on the strain rate and has no memory of its initial configuration). The viscoelastic properties of cell membranes have already been characterised, for erythrocytes in particular (Evans & Hochmuth, 1976; Hochmuth & Waugh, 1987). It is thus, quite likely that supported bilayers also show viscoelastic properties.

When subjected to stress, viscoelastic materials dissipate the applied stress owing to their viscous properties. They do so in a characteristic time scale referred to as their 'relaxation time'. Depending on the how the timescale of perturbation of the system scales with respect to this intrinsic relaxation time, the material can show mostly viscous or mostly elastic behaviour (Barnes et. al., 2005). At perturbation time scales lower than the relaxation time, one observes elastic behaviour, whereas for perturbation time scale higher than the relaxation time, one observes viscous behaviour. Hence, if the membrane tether is a viscoelastic material (membrane tethers pulled from cell membranes have been shown to be viscoelastic in work by Schmitz et. al., 2007), changing the time scale of perturbation of this tether should lead to an observable effect.

The tether pulling rate variation experiments can be interpreted in this paradigm. If steps reflect stick-slip motion of the bilayer, at higher pulling rates, i.e. low timescale perturbation, the membrane should show elastic behaviour and a greater probability of stick-slip motion, whereas at lower pulling rates i.e. large timescale perturbation, the membrane should show viscous behaviour and a lower probability of stick slip motion. In accordance with this hypothesis, in experiments done on cell membranes and supported bilayers, the frequency of occurrence of steps (step probability) shows an increasing trend with increasing pulling rates.

Our stick-slip hypothesis for the step wise relaxation takes into consideration a membrane-only response to tether pulling, but the mechanical response of cell membranes to tether pulling might be quite complicated. This is already reflected in the presence of two distinct kinds of step wise relaxations in cell membranes. Hence, we remain open to possibilities about the origin of the step wise relaxation in cell membranes. These possibilities range from a response involving only the lipid bilayer to one involving the cortical actin cytoskeleton and its interaction with the plasma membrane via integral membrane proteins or a more local unfolding of membrane proteins.

Estimation of the actual stress relaxation time of these tethers was also attempted. A common challenge faced while carrying out the relaxation time estimation experiment was reaching the attractive set point after which tether relaxation was to be observed. Due to technical limitations, this set point is not reached accurately. This may have an effect on the force traces observed during the force pause when cantilever movement is stopped. In the case of cell membranes, the relaxation profiles observed did not conform to standard decay fits (exponential or an empirical $t/(1+t)$), and hence could not be used to determine the actual system relaxation time. In the case of supported bilayers, the relaxation often occurred before the attractive set point was reached. The typical relaxation of tethers pulled from supported bilayers also occurred quite fast, such as even at the highest sampling rate allowed by the instrument, the data density in the relaxation trace was low and could not be fitted to a standard decay fit.

The magnitude of the stepwise relaxation remains fairly constant with pulling rate in supported bilayers, but increases with increasing pulling rates in cell membranes.

However, we do not understand the significance of the magnitude of the step height or its dependence on pulling rate yet.

(iii) Pulling rate dependence of tether force

Tether forces measured in force curves show a clear, non-linear rate dependence in both cell membranes and glass supported bilayers. In these experiments, the minimum of the force curve (at the 'dip') is taken as a measure of the tether force. This force contains the force required to form a membrane tether, but could also include adhesion forces to the membrane surface. There is no straightforward way to decompose these two components of the tether force.

In tethers pulled using optical tweezers from cell membranes of neuronal growth cones, a linear dependence of the tether force on the tether extraction speed has been reported; tether diameter is known to remain constant in this process (Dai & Sheetz, 1995). However, the tether force measured in these experiments is different from that measured in our AFM based force spectroscopy experiments. The nature of the tether pulling force curves obtained via force spectroscopy experiments and optical tweezer experiments is quite different as mentioned before. Hence, while the minimum in the retraction force curve (while the tether is being pulled and force equilibrium is not reached) is taken to be an estimate of the 'tether force' in our force spectroscopy experiments, the plateau force (corresponding to the steady state of force on the tether, after the initial steep increase in force) is considered for the same purpose in optical tweezer experiments. Also, the range of tether extraction velocities in this pulling rate variation experiment is smaller (0 – 20 $\mu\text{m/s}$) compared to the range of pulling rates in our experiments (0.1 – 100 $\mu\text{m/s}$).

Given the linearity of the tether force – tether velocity plot, this tether force rate dependence is thought to result from viscous slippage of the cell membrane on the cytoskeleton. Hochmuth et. al. (Hochmuth & Sheetz, 1996) show that the contribution of the bilayer-cytoskeleton slippage outweighs the contribution of membrane viscosity and interbilayer slip. They also show that a similar linear tether force rate dependence obtained on unilamellar vesicles (Evans & Yeung, 1994) can be explained in terms of interbilayer slip.

In a similar set of rate dependence experiments performed on outer hair cells, by pulling membrane tethers with optical tweezers, Li et. al. (2002) actually distinguish between the steeply increased (peak) force required to form the tether and the steady state force achieved after the formation of the tether. Also, in these experiments, pulling rates were changed on the same tether in order to reduce experimental variability. The tether force trend reported in these experiments also varies linearly with the pulling rate and is explained using the model proposed by Hochmuth et. al.

A recent study (Brochard –Wyart et. al., 2006) uses a different model to explain the tether force rate dependence trends reported by Dai et. al. and Li et. al. They propose that the change in observed tether force with pulling rate can be explained on the basis of a change in tether radius with pulling rate. They show that this model, based on narrowing of the tether at a higher pulling rate fits well to reported data. Their model takes into consideration the different effects of integral membrane proteins and the cortical cytoskeleton on membrane flow at different tether pulling rates.

Coming back to the results in our experiments, we see a qualitatively similar non linear rate dependence of the ‘dynamic’ tether force for both cell membranes and supported bilayers. This suggests that this rate dependence might represent another intrinsic property of the lipid bilayer. Since these trendlines are non-linear, viscous behaviour of the bilayer can not account for them. Instead a viscoelastic response, where the bilayer gains increasingly elastic character with increasing pulling rates and stiffens, could result in such a non linear trend with an inflection.

These trendlines show a sudden increase in slope within a narrow range of pulling rates. Below an ‘onset’ rate, the tether force does not vary much with pulling rate, but above the onset, it varies faster. What determines this onset rate is a question of interest to us. We hypothesise that the onset rate is determined by a parameter of the intrinsic timescale of the relaxation of lipids in bilayers. This is based on the idea that the change in pulling rate changes the time scale of perturbation of lipid molecules (where lipids have to reorganise and rearrange while a tether is being formed) with respect to their intrinsic time scale of thermal motion. One parameter of this intrinsic thermal motion is the diffusion coefficient. It is known that the ‘average’

diffusion coefficient of lipids in supported bilayers is 5 – 100 fold higher than the diffusion coefficient of lipids in cell membranes (Sonnleitner et. al., 1999, Lee et. al., 1993). Given that the onset rates of tether force rate dependence in supported bilayers are generally higher than that of cell membranes, we feel that this intrinsic relaxation time scale may be determined by the diffusion coefficient of membrane lipids. We plan to carry out experiments and measure the diffusion coefficient of labelled lipids in cell membranes and supported bilayers, in order to throw more light upon the nature of the rate dependence of tether force.

While tether force rate dependence has been studied before and rationalised with various models, in our opinion, the presence of a viscoelastic response could point towards a change in material characteristics of lipid membranes with a change in the rate of deformation. In literature, (steady state) tether force has already been related to bending stiffness of bilayers (Hochmuth et. al., 1996). The change in such a material property of a membrane is quite an exciting possibility as it may have implications for the membrane deformation processes occurring intracellularly at different rates, such as endocytosis and actin-mediated cell protrusion during migration. Hence, such a change in basic physical character of the membrane with deformation rate opens up yet another regulatory handle for modulating membrane function.

5. References

Apodaca, G (2002) Modulation of membrane traffic by mechanical stimuli. *AJP - Renal Physiol.* 282 :F179-F190.

Banks HT, Hu S and Kenz ZR (2011) A Brief Review of Elasticity and Viscoelasticity for Solids. *Adv. Appl. Math. Mech.*, 3(1): 1-51

Baoukina S, Marrink SJ, Tieleman DP (2012) Molecular structure of membrane tethers. *Biophys J.*102(8):1866-71.

Barnes HA, Hutton JF and Walters K (2005) *An Introduction to Rheology.* Elsevier Ltd.

Bo L and Waugh RE (1989) Determination of bilayer membrane bending stiffness by tether formation from giant, thin-walled vesicles. *Biophys J.*55:509–517.

Brochard-Wyart F, Borghi N, Cuvelier D, Nassoy P (2006) Hydrodynamic narrowing of tubes extruded from cells. *Proc Natl Acad Sci U S A.*103(20):7660-3.

Dai J and Sheetz MP (1995) Mechanical properties of neuronal growth cone membranes studied by tether formation with laser optical tweezers. *Biophys J.* 68: 988–996

Dai J and Sheetz MP (1998) Cell membrane mechanics. *Methods Cell Biol.* 55: 157–171.

Dai J, Sheetz MP (1995) Regulation of endocytosis, exocytosis, and shape by membrane tension. *Cold Spring Harb Symp Quant Biol.* 60:567-71.

Dai, J, Ting-Beall, HP, Sheetz, MP (1997) The secretion-coupled endocytosis correlates with membrane tension changes in RBL 2H3 cells. *J Gen Physiol.* 110: 1-10.

Diz-Muñoz A, Fletcher DA, Weiner OD (2013) Use the force: membrane tension as an organizer of cell shape and motility. *23(2):47-53*

Evans E (1973) New membrane concept applied to the analysis of fluid shear and micropipette deformed red blood cells. *Biophys J. 13 : 941–954.*

Evans, EA and Hochmuth, RM (1976) Membrane viscoelasticity. *Biophys J.16:1-11*
Fujiwara T, Ritchie K, Murakoshi H, Jacobson K, Kusumi A (2002) Phospholipids undergo hop diffusion in compartmentalised cell membrane. *J Cell Biol. 157(6):1071-81.*

Hénon S, Lenormand G, Richert A, and Gallet F (1999) A new determination of the shear modulus of the human erythrocyte membrane using optical tweezers. *Biophys J.76:1145– 1151.*

Hochmuth FM, Shao JY, Dai J, Sheetz MP (1996) Deformation and flow of membrane into tethers extracted from neuronal growth cones. *Biophys J. 70(1):358-69.*

Hochmuth R and Waugh R (1987) Erythrocyte membrane elasticity and viscosity. *Annu. Rev. Physiol. 49:209–219*

Hochmuth R and Waugh, R (1987) Erythrocyte membrane elasticity and viscosity. *Annu. Rev. Physiol. 49: 209–219.*

Hochmuth RM, Mohandas N, Blackshear, PL (1973) Measurement of the elastic modulus for red cell membrane using a fluid mechanical technique. *Biophys J. 13:747-62.*

Hochmuth RM, Wiles HC, Evans EA, McCown JT (1982) Extensional flow of erythrocyte membrane from cell body to elastic tether. II. Experiment. *Biophys J. 39(1): 83–89.*

Hochmuth RM., Wiles HC., Evans EA, McCown, JT (1982) Extensional flow of erythrocyte membrane from cell body to elastic tether: II. Experiment. *Biophys J.* 39:83-89.

Hutter JL and Bechhoefer J (1993) Calibration of atomic force microscope tips. *Rev. Sci. Instrum.* 64:1868-73.

Inaba T, Ishijima A, Honda M, Nomura F, Takiguchi K, Hotani H (2005) Formation and maintenance of tubular membrane projections require mechanical force, but their elongation and shortening do not require additional force. *J Mol Bio.* 348(2):325-33.

Keren, K (2011) Membrane tension leads the way. *Proc Natl Acad Sci U S A.* 108(35): 14379–14380.

Kocun M, Lazzara TD, Steinem C, Janshoff A (2011) Preparation of solvent-free, pore spanning lipid bilayers : modeling the low tension of plasma membranes. *Langmuir.* 27(12):7672-80.

Kocun M and Janshoff A (2012) Pulling tethers from pore spanning bilayers : towards simultaneous determination of local bending modulus and lateral tension of membranes. *Small.* 8(6):847-51.

Kuo SC and Sheetz MP (1992) Optical tweezers in cell biology. *Trends Cell Biol.* 2(4):116-8.

Lee GM, Zhang F, Ishihara A, McNeil CL, Jacobson KA (1993) Unconfined lateral diffusion and an estimate of pericellular matrix viscosity revealed by measuring the mobility of gold tagged lipids. *J Cell Biol.* 120 (1) : 25- 35.

Li Z, Anvari B, Takashima M, Brecht P, Torres JH, Brownell WE (2002) Membrane tether formation from outer hair cells with optical tweezers. *Biophys J.* 82(3):1386-95

Morris E, Homann U (2001) Cell surface area regulation and membrane tension. *J Membr Biol.* 179(2):79–102.

Müller DJ, Helenius J, Alsteens D, Dufrêne YF (2009) Force probing surfaces of living cells to molecular resolution. *Nat Chem Biol.* 5(6):383-90.

Neuman KC and Block SM (2004) Optical trapping. *Rev Sci Instrum.* 75(9):2787-809.

Pontes B, Viana NB, Salgado LT, Farina M, Moura Neto V, Nussenzveig HM (2011) Cell cytoskeleton and tether extraction. *Biophys J.* 101(1):43-52.

Pucadyil TJ and Schmid SL (2010) Supported bilayers with excess membrane reservoir: a template for reconstituting membrane budding and fission. *Biophys J.* 99(2):517-25

Raucher D and Sheetz MP. (1999), Characteristics of a membrane reservoir buffering membrane tension. *Biophys J.* 77:1992 - 2002.

Raucher D and Sheetz MP (2000) Cell spreading and lamellipodial extension rate is regulated by membrane tension. *J Cell Biol.* 148:127-36.

Raucher D, Stauffer T, Chen W, Shen K, Guo S, York JD, Sheetz MP, Meyer T (2000) Phosphatidylinositol 4,5-bisphosphate functions as a second messenger that regulates cytoskeleton-plasma membrane adhesion. *Cell.* 100(2):221-8.

Schmitz J, Benoit M, Gottschalk KE (2008) The viscoelasticity of membrane tethers and its importance for cell adhesion. *Biophys J.* 95(3):1448-59.

Sheetz, MP and Dai, J (1996) Modulation of membrane dynamics and cell motility by membrane tension. *Trends Cell Biol.* 6:85-89.

Sonnleitner A, Schutz GJ, Schmidt Th. (1999) Free Brownian motion of individual

lipid molecules in biomembranes. *Biophys J.* 77 : 2638 – 42.

Staykova M, Arroyo M, Rahimi M, Stone HA. (2013) Confined bilayers passively regulate shape and stress. *Phys Rev Lett.* 110(2):028101.

Staykova M, Holmes DP, Read C, Stone HA (2011) Mechanics of surface area regulation in cells examined with confined lipid membranes. *Proc Natl Acad Sci U S A.* 108(22):9084-8.

Sun M, Graham JS, Hegedüs B, Marga F, Zhang Y, Forgacs G, Grandbois M (2005) Multiple membrane tethers probed by atomic force microscopy. *Biophys J.*89(6):4320-9.

Sun M, Northup N, Marga F, Huber T, Byfield FJ, Levitan I, Forgacs G (2007) The effect of cellular cholesterol on membrane-cytoskeleton adhesion. *J Cell Sci.* 120:2223-31.

Waugh RE, Song J, Svetina S, Zeks B (1992) Local and nonlocal curvature elasticity in bilayer membranes by tether formation from lecithin vesicles. *Biophys J.* 61:974–982.

